2014

Quenching of Tryptophan Fluorescence in Various Proteins by a Series of Small Nickel Complexes

Heather F. Crouse
Susquehanna University

Julianne Potoma
Susquehanna University

Farhat Nejrabi
Penn State Harrisburg

Deanna L. Snyder
Susquehanna University

Balwant S. Chohan
Penn State Harrisburg

See next page for additional authors

Recommended Citation

Alexander A. Rhodes, Brandi L. Swartz, Erik R. Hosler, Deanna L. Snyder, Kristen M. Benitez, Balwant S. Chohan and Swarna Basu, Static quenching of tryptophan fluorescence in proteins by a dioxomolybdenum(VI) thiolate complex, J. Photochem. Photobiol. A 293, 81 (2014).

Quenching of Tryptophan Fluorescence in Various Proteins by a Series of Small Nickel Complexes

Heather F. Crouse[1], Julianne Potoma[1], Farhat Nejrabi[2], Deanna L. Snyder[1], Balwant S. Chohan[2] and Swarna Basu[1]*

[1] Department of Chemistry, Susquehanna University, 514 University Avenue Selinsgrove, PA 17870

[2] Current address: Penn State Harrisburg, 777 West Harrisburg Pike, Middletown, PA 17057

* Corresponding author. Tel.: 1-570-372-4223; Fax: 1-570-372-2752

E-mail address: basu@susqu.edu

ABSTRACT

A series of twelve anionic, cationic, and neutral nickel (II) complexes have been synthesized and characterized. The interaction of these complexes with bovine serum albumin (BSA), human serum albumin (HSA), lysozyme (Lyso), and tryptophan (Trp) has been studied using steady-state fluorescence spectroscopy. Dynamic and static quenching constants have been calculated, and the role played in quenching by the ligand and complex charge investigated. The nickel complexes showed selectivity towards the different proteins based on the environment surrounding the Trp residue(s). Only small neutral complexes with hydrophobic ligands effectively quenched protein fluorescence *via* static quenching, with association constants ranging from 10^2 M^{-1} (free Trp) to 10^{10} M^{-1} (lysozyme), indicating a spontaneous and thermodynamically favorable interaction. The number of binding sites, on average, was determined to be one in BSA, HSA and free Trp, and two in lysozyme.

Keywords:

Transition metal complexes

Serum albumins

Static and dynamic quenching

FRET

INTRODUCTION

Protein interactions play a fundamental role in many biochemical processes in both the healthy and the diseased state, including critical roles in signal transduction, immune reaction, cell cycle control, differentiation, and protein folding. In order to understand, probe and manipulate biological systems effectively there is a need to develop small molecules that influence or inhibit protein interactions through selective recognition.[1,2] Small metal complexes can potentially combine flexibility in ligand design with access to a wide and diverse range of coordination geometries, optical isomers and electronic states. This flexibility can be used to enable or prevent coordination of the metal complex to protein side chains or substrates.

a. Serum Proteins: Several different transport proteins exist in blood plasma, but only albumin is able to bind and transport a wide diversity[3-6] of ligands with reversibility and high affinity. For many drugs, binding to serum albumin is a critical determinant of their distribution and pharmacokinetics.[7-9] HSA accounts for 60% of the measured serum proteins, thus one of the most abundant proteins in the circulatory system.[10-13] HSA consists of a single polypeptide chain of 585 amino acids, a scarcity of Trp and Met residues, and an abundance of Cys and charged residues.[14-17] BSA is a homologous globular protein, consisting of 583 amino acid residues in the mature form, the sequence of BSA is 76% identical to that of HSA. While the crystal structure of HSA as well as its binding with fatty acids has been characterized, the crystallographic structure of BSA has not been determined to any sufficient resolution.[16-19] The albumins are composed of three structurally similar domains (I, II and III), each containing two subdomains (A and B) and stabilized by 17 disulphide bridges.[11-15,20-24] The flexible multidomain structures house a variety of binding sites, and allows for cooperativity and allosteric modulation, thus making HSA and BSA similar to multimeric proteins.

Albumins can reversibly bind with a number of molecules in the plasma through various interactions. Of the two major structurally selective binding sites, the binding affinity offered by site I is largely through hydrophobic interactions, whereas site II involves a combination of hydrophobic, hydrogen bonding, and electrostatic interactions.[25,26] Most strongly bound are medium-sized hydrophobic organic anions, including long-chain fatty acids, bilirubin and haematin. Hydrated monovalent cations do not associate to any significant extent, whereas hydrated divalent cations such as Ca^{2+} strongly bind at select groups on the albumin molecule.[27] Information about the interaction of ions surrounded by various types of organic ligands with serum albumin can help reveal the role of albumins in the normal state and in the diseased state, and thus provide the basis for the rational-design of efficient drugs, sensitizers, and new therapeutic approaches.

b. Nickel and Metal Binding: Metals have important roles in biological systems ranging from essential to toxic, and as such the metal-binding capacity of albumins has been widely studied over the years,[28-33] including the affinity, stoichiometry and specificity of Ca(II), Co(II), Ni(II), Cu(II), Zn(II), Cd(II), Cr(III), V(III), and Mo(VI) ions.[34-46] Although there is a lack of detailed structural information, four different metal sites have been described, and specificity is achieved by exploiting differences in the co-ordination chemistries of the preferred metal ions: (i) ATCUN site (N-terminal Cu/Ni-binding) motif at the N-terminus, the primary site[47] for Cu(II) and Ni(II); (ii) site A, the

primary Zn(II)-binding site[6] that can also bind other +2 metal ions; (iii) site B, which displays a high affinity towards Cd(II), the location of which is unknown;[36,38,40] and (iv) the reduced thiol of Cys-34, which binds gold[48] and platinum[49,50] compounds.

Nickel enzymes were first discovered[51] in the 1970's, and although studies in rats indicates that Ni is an essential element for higher animals,[52,53] neither the source of the Ni requirement nor a single mammalian Ni-dependent enzyme has been identified. Although pure Ni itself is not toxic, Ni complexes can be highly toxic especially with long term contact exposure in humans.[54,55] Allergy to Ni is a phenomenon which has assumed growing importance in recent years.[56] According to current models, haptens penetrating the epidermis bind to carrier proteins found just under the skin, leading to an inflammatory reaction within the skin.[57-63] The role played by albumins in translocating Ni^{2+} toward deeper epidermal layers has not been satisfactorily resolved, though it is of interest that (1) HSA is particularly abundant in skin, (2) it is a transporter of essential nutrients for epithelial cells in the absence of blood vessels, and (3) it is able to efficiently cross the epidermal basement membrane.[64] The investigation of the interaction of Ni complexes with serum albumins is imperative.

c. Fluorimetry: One way to measure the extent and accessibility of protein binding sites to small molecules involves fluorescence quenching. Information concerning the number of binding sites, the binding constant K_a, and the distance between donor and acceptor can be readily obtained using Stern–Volmer kinetics and Forster's theory.[65-68] The fluorescence signature of a protein derives from the aromatic residues. The fluorescence from the indole group in Trp is extremely sensitive to its environment, and is a convenient spectroscopic probe for the structure and rotational dynamics surrounding the Trp residue.[66,69] These Trp residues can undergo electronic excitation in the visible region, and the emission can be quenched *via* different mechanisms depending on the degree of "exposure" to the quencher.[70,71] Therefore, changes in the intrinsic fluorescence and the bimolecular quenching rate constant can be used to monitor structural changes in a protein, and reveal information on Trp accessibility and how deep it is buried in the protein.[66] In HSA, a Trp residue at position 214 is buried in the second helix of the second domain, in a hydrophobic fold. BSA has an additional Trp in position 131 which is found on the surface of the protein.[13]

The interaction of metal ions has led to our interest in studying the interaction of transition metal complexes with proteins. The primary focus has been on the effect that different ligand systems have on the interaction, particularly the drug-binding sites of BSA. Secondly, the possibility that fluorescence quenching of the protein is due to FRET (fluorescence resonance energy transfer) from the protein to the complex will lead to the calculation of intermolecular distances to help determine the proximity of the complex to the albumin proteins.[13] A recent study concerning the interaction of a fluorone-Mo(VI) complex with HSA and BSA[72] showed strong and significant interactions between the metal complex and the protein.[73] Others have recently reported that a Cr(III) complex, ($[Cr(salprn)(H_2O)_2]ClO_4$), is capable of quenching BSA *via* FRET leading to a non-specific photocleavage of the protein.[74,75] We have recently shown that a Cr(III) complex, (R,R)-N,N'-Bis(3,5-di-tert-butylsalicylidene)-1,2-cyclohexane-diamino chromium (III), binds very tightly to serum albumins and lysozyme, and that the binding is highly specific and the quenching is static in

nature and is not due to energy transfer.[76] Lysozyme is included in our studies since it is well characterized,[77-79] and contains multiple Trp residues that are important for enzymatic activity.[80] It is a single polypeptide chain of 129 amino acid residues, six of which are Trp residues at positions 28, 62, 63, 108, 111, and 123. The residues at 62, 63, and 108 are located deep in the active site. It is expected that each of the residues will be affected differently depending upon their accessibility, and thus contributing independently to the inherent fluorescence intensity.[71,77,80-83]

In this work, we have studied the interaction between a series of Ni (II) complexes (**Figure 1**) and Lysozyme, HSA and BSA, using fluorescence and UV–vis spectroscopic techniques under physiological conditions. The interaction between the Ni (II) complexes and free Trp was also investigated to illustrate the affinity of the complex for this particular amino acid residue, irrespective of environment. The results have allowed us to discuss the type, degree and nature of the interaction and binding between the protein and metal complexes with consideration to polarity, hydrophobicity, charge, and spin state of the metal complex.

EXPERIMENTAL

A. General Procedures

Unless otherwise mentioned, all chemicals were of analytical reagent grade (Sigma Aldrich or VWR). Synthetic procedures and manipulations were conducted using Schlenk techniques, under an Ar atmosphere. The solvents were either HPLC-grade or were dried and distilled using conventional[84,85] methods and stored under an Ar atmosphere. All proteins and Trp were purchased from Sigma-Aldrich and used without further purification. Stock solutions of proteins, Trp and Ni(II) complexes were prepared in 50 mM Tris–HCl buffer solution (pH 7.4). Synthesis and characterization data for all complexes (except for pertinent X-ray crystallography data) is reported in the **SI (#1)**.

B. Physical Measurements – Characterizations.

NMR spectra were recorded at room temperature on a Anasazi-Varian 60 MHz FT spectrometer at Penn State Harrisburg, or a Bruker AC200 FT at UMass-Amherst, or a Bruker 500MHz FT spectrometer at Penn State Hershey Medical Center. Chemical shifts are reported in ppm relative to internal standard of TMS. FTIR data for solid samples (as KBr disks) and liquid samples (neat) were obtained on a Jasco 4000 or a Perkin Elmer 783 IR spectrometer. The IR spectral peaks were calibrated with polystyrene, and are reported in wavenumbers. Relative intensities of the bands in a spectrum are indicated (w = weak, m = medium, s = strong, vs = very strong, br = broad). Solid-state magnetic susceptibilities were obtained on Johnson Matthey (MK-1 and MSB-1) magnetic susceptibility Gouy balances. The Evans technique for measurement of solution magnetic moments was also employed,[86,87] using coaxial NMR tubes. Electrospray mass spectrometry (ESI-MS and $(MS)^n$) measurements were made at UMass using an Esquire LC/MS 32 instrument, or at Penn State using an Applied Biosystems API 150EX instrument. The m/z values are given to 4 significant figures. The reported m/z values in the synthetic section correspond to the most intense peak in the

isotopic cluster, the calculated & theoretical m/z values are based on isotopic masses (on the weight of the most common isotopes, monoisotopic mass). In some cases the 'most intense peak' value and the calculated 'common isotope' value may not necessarily be the same. Samples for ESI-MS analysis were introduced as MeOH/MeCN solutions, and routinely characterized in a combination of both positive and negative modes. Isotopic MS clusters were identified, and all those highlighted were found to be in accordance with their simulations. Selected simulated spectra and the regions that they represent in the original spectra are included in the **SI**. Spectra were simulated using various MS calculating software programs. Appropriate coupled MS/MS and $(MS)^n$ methods were utilized where necessary, and both the parent spectra and the fragmentation patterns were used to elucidate the reaction products. The experimental data indicate the successful preparation of the complexes mentioned. Elemental analyses were performed at the UMass-Amherst Microanalysis Center, and QTI, Whitehouse, NJ. Samples for microanalysis were ground to a fine powder and vacuum desiccated over phosphorus pentoxide prior to analysis.

Single-crystal X-Ray crystallographic studies were performed in part by Dr. Carl Carrano and Mr. J. Hoffman at San Diego State University using a Bruker X8 Apex diffractometer (**Complex 2)**, by Dr. H. Yennawar using a Bruker Apex SMART CCD diffractometer at Penn State University (**Complex 3, 8, 10)**, and by Dr. A. Chandrasekaran at UMass-Amherst using a Nonius Kappa CCD diffractometer (**Complex 6**). For each apparatus, a graphite monochromated Mo K_α radiation (λ = 0.71073Å) source was employed. Data were generally collected at 23 ± 2°C, specific details are given in the **SI**. A θ-2θ scan mode was used for data collection from about $2° \leq 2\,\theta_{Mo\ K\alpha} \leq 29°$. The data were solved by a full matrix least squares refinement on F^2 using the SHELX suite of programs.[88] The plotting program ORTEP-3 for Windows or CaChe-6 (Fujitsu Ltd, 2004) was used[89] for the structural diagrams:

Complex 2: The crystal used to solve complex **2** was a red colored plate (BSC1a) with approximate dimensions 0.2 x 0.2 x 0.02 mm^3. A total of 10794 independent reflections were collected at **200K**, and final refinement was based on 6246 observed reflections ($I \geq 2\sigma_i$). Sum formula is $NiC_{11}H_{24}N_2S_2$. FW is 307.15. Crystals of **2** form in the monoclinic space group $P2_1/n$ with cell dimensions a = 10.5547(10) Å, b = 12.3943(11) Å, c = 11.5831(11) Å. $\alpha = \gamma = 90°$, β = 111.126(5)°, and Z = 4. R_{int} = 0.087. The structure was refined to R = 4.40% and R_w = 10.22% ($I > 2\sigma(I)$). Pertinent crystallographic data is provided in **Table 1**. Details are provided in **SI (#2)**.

Complex 3: The crystal used to solve complex **3** was blue block (BTW5s) with approximate dimensions 0.21 x 0.32 x 0.37 mm^3. A total of 7086 independent reflections were collected at 298K, and final refinement was based on XYZ centroids of 6974 reflections above 20 σ(I) with $2.320° < \theta < 28.167°$. Sum formula is $NiC_{17}H_{40}I_2N_4O_4S_2$. FW is 741.16. Crystals of **3** form in the triclinic space group P-1 with cell dimensions a = 10.4046(12)Å, b = 10.9123(12)Å, c = 13.8838(16)Å, α = 87.671(2)°, β = 78.132(2)°, γ = 72.023(2)° and Z = 2. R_{int} = 0.013. The structure was refined to R = 4.90% and R_w = 13.86% ($I > 2\sigma(I)$). Pertinent crystallographic data is provided in **Table 1**. Details are provided in **SI (#3)**.

Complex 6: The crystal used to solve complex **6** was a blue colored plate (BC39) with approximate dimensions 0.15 x 0.15 x 0.05 mm^3. A total of 3113 independent reflections were collected at 293K, and final refinement was based on 2038 observed reflections ($I \geq 2\sigma_i$). Sum formula is $NiC_{13}H_{28}I_2N_4O_2S_2$. FW is 649.02. Crystals of **6** form in the monoclinic space group P2(1)/n with cell dimensions a = 11.2811(9) Å, b = 12.8465(8) Å, c = 15.4674(13) Å. α = γ = 90°, β = 83.251(4)° and Z = 4. R_{int} = 0.1173. The structure was refined to R = 6.41% and R_w = 13.83% (I > 2σ(I)). Pertinent crystallographic data is provided in **Table 1.** Details are provided in **SI (#4)**.

Complex 8: The crystal used to solve complex **8** was blue-purple colored plates (BTW17o) with approximate dimensions 0.30 x 0.02 x 0.02 mm^3. A total of 3752 independent reflections were collected at 298K, and final refinement was based on 3556 observed reflections ($I \geq 2\sigma_i$). Sum formula is $NiC_{10}H_{19}N_2O_{12}$. FW is 417.96. Crystals of **8** form in the orthorhombic space group Pna2(1) with cell dimensions a = 14.669(5) Å, b = 16.306(5) Å, c = 7.034(2) Å. α = γ = β = 90°, and Z = 4. R_{int} = 0.029. Flack parameter = 0.047 (8). The structure was refined to R = 3.68% and R_w = 9.41% (I > 2σ(I)). Pertinent crystallographic data is provided in **Table 2.** Details are provided in **SI (#5)**.

Complex 10: The crystal used to solve complex **10** was a red-pink colored plate (BSC1o) with approximate dimensions 0.01 x 0.12 x 0.22 mm^3. A total of 1650 independent reflections were collected at 298K, and final refinement was based on XYZ centroids of 915 reflections above 20 σ(I) with 2.248°<θ<24.842°. Sum formula is $NiC_{10}H_{22}N_2S_2$. FW is 293.13. Crystals of **10** form in the orthorhombic space group Pbcn with cell dimensions a = 9.487(6) Å, b = 7.862(5) Å, c = 18.145(13) Å. α = β = γ = 90°, and Z = 4. R_{int} = 0.0863. The structure was refined to R = 6.32% and R_w = 14.51% (I > 2σ(I)). Pertinent crystallographic data is provided in **Table 1.** Details are provided in **SI (#6)**.

C. Physical Measurements - Quenching Experiments

UV-visible absorbance measurements (UV-vis) were obtained on a HP 8453 Diode Array Spectrometer, or a Cary 4000 UV-vis Spectrophotometer. All experiments were performed at room temperature. The fluorescence emission spectra were obtained using a PE LS50B Spectrometer. Fluorescence spectra were normalized and then corrected for wavelength dependent sensitivity using a calibration curve generated using five spectral fluorescence standards (BAM-F001 to F005, Sigma-Aldrich).[90] For each series, the protein (or free Trp) concentration was held constant at 1.0 x 10^{-5} M and the concentration of each Ni(II) complex was varied (0.0 μM to 21.0 μM) through the preparation of individual samples. The excitation wavelength was 280 nm, emission wavelength was 345 nm and excitation and emission slit widths were 3.5 nm each. The dynamic quenching constants were determined using the Stern-Volmer equation [67,71]:

$$\frac{F_0}{F} = 1 + K_{SV}[Q] \quad (1)$$

F_0 and F correspond to the fluorescence intensities of the protein without quencher and in the presence of quencher, respectively. $[Q]$ is the concentration of the quencher and K_{SV} is the Stern-Volmer quenching constant. Also, K_{SV} is related to the lifetime of the system according to **equation 2** [67]:

$$K_{SV} = k_q \tau_0 \quad (2)$$

k_q is the bimolecular quenching constant and τ_0 is the lifetime of unquenched fluorophore. τ_0 is short for Trp alone (2.7 ns) but longer in a protein environment (9.8 ns). [91-93] The static quenching constant, also known as the binding constant, K_a, and number of binding sites (n) between the protein and metal complexes were calculated using **equation 3** [67,94]:

$$log\left[\frac{F_0 - F}{F}\right] = logK_a + nlog[Q] \quad (3)$$

The modified Stern-Volmer plot is useful when studying a protein that has Trp in different environments, for example buried residues *versus* residues at the surface, as is the case with both BSA and lysozyme.[66,67] In such cases the Stern-Volmer plot will have a downward curve indicating that some of the fluorescence is not accessible. In this study, the modified Stern-Volmer analysis was not relevant as the complexes were quenching the proteins and free Trp *via* static quenching.

RESULTS & DISCUSSION

The series of small water soluble Ni(II) complexes (**Figure 1**) represents molecules that vary in charge (neutral, cationic, anionic), spin state (low, high), and degree of hydrophilicity by virtue of the nature of ligands.

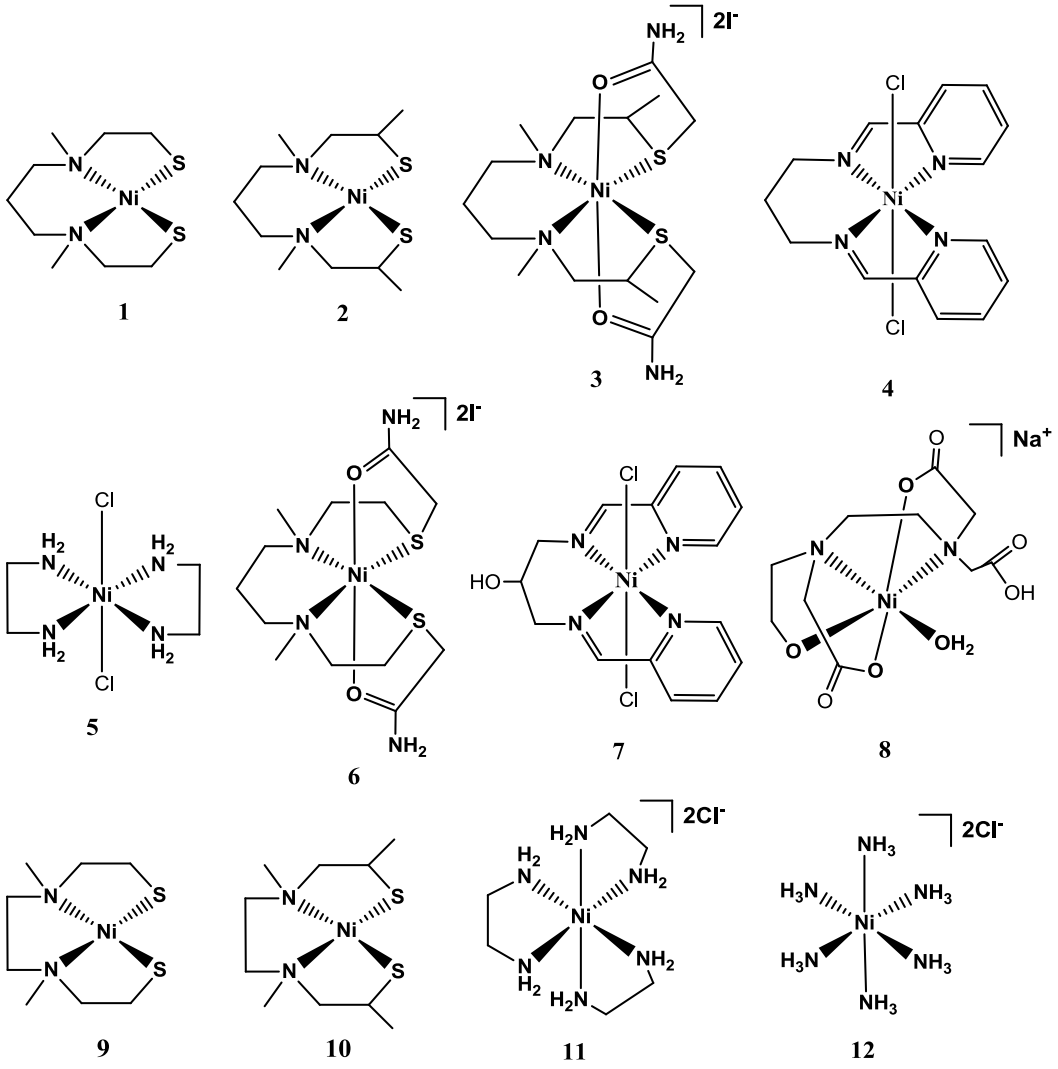

Figure 1. Ni(II) complexes used in this study, I. Ni-Pr-Et. II. Ni-Pr-Pr. III. Ni-Pr-Pr-Iodo. IV. $Ni(pya_2tn)Cl_2 \cdot H_2O$. V. $Ni\text{-}(en)_2Cl_2$. VI. Ni-Pr-Et-Iodo. VII. $Ni(pya_2tn\text{-}OH)Cl_2$. VIII. $Ni(EDTA)\text{-}H_2O\text{-}Na$ IX. Ni-Et-Et. X. Ni-Et-Pr. XI. $Ni(en)_3Cl_2.2H_2O$ XII. $Ni(NH_3)_6Cl_2$. [(Pr = propyl, Et = ethyl, en = ethylenediamine, tn = trimethylene diamine, EDTA = ethylenediaminetetraacetate, pya = Schiff base ligand derived from pyridine-2-carboxaldehyde and 1,3-diaminopropane (pya_2tn)]

A. Synthesis and Characterizations of the Nickel Complexes

Complexes 1, **2**, **9**, and **10**: These four Ni(II) compounds are *cis* diamino dithiolate square planar complexes. Sulfur containing ligands readily form $[NiL_2]^{2-}$ type four coordinate complexes in the presence of large excess of dithiolato ligand (L_2). At lower ligand concentrations, the propensity of thiolato-S to form bridges between metal centers gives rise to multinuclear species, an inconvenience that is also dependent on reaction conditions, such as temperature and protic solvent conditions.[95,96] One way to prevent such oligomerizations is to use bulky and/or aromatic substituents and/or chelate ligands that readily undergo template reactions. The latter method was used to synthesize four of the

complexes reported herein. The synthesis of each of the low spin neutral complexes **1**, **2**, **9**, and **10** are analogous (**SI #1).** Complexes **1** and **9** have been previously synthesized, and crystal structures reported.[95,97,98] All characterization data, including ESI-MS spectra and elemental microanalysis are consistent with the formulations and structures given for each complex (see **SI #1**). Selected bond lengths and angles for **1**, **2**, **9**, and **10** are given in **Table 1**. The molecular structures of each of these four complexes reveal discreet mononuclear units, with no intermolecular Ni-S interactions.

Table 1: A comparison of selected bond lengths (Å) and bond angles (°) for complexes **1**,[97] **6**, **2**, **3**, **9**,[98] and **10**.

Bond Lengths (Å)						
	1	**6**	**2**	**3**	**9**	**10** ⊾
Ni-S1	2.176(1)	2.407(4)	2.1605(3)	2.4406(12)	2.166(1)	2.1679(16)
Ni-S2	2.174(1)	2.446(3)	2.1692(3)	2.4319(11)	2.173(1)	2.1679(16)
Ni-N1	1.999(3)	2.098(10)	1.9888(9)	2.121(3)	1.931(4)	1.939(4)
Ni-N2	2.006(3)	2.118(10)	1.9844(9)	2.128(4)	1.942(4)	1.939(4)
Ni-O1		2.134(8)		2.042(3)		
Ni-O2		2.035)8)		2.063(3)		
Bond Angles (°)						

S1-Ni-S2	85.37(4)	96.00(12)	88.044(14)	91.32(4)	94.01(6)	96.18(9)
S1-Ni-N1	89.31(9)	87.6(3)	88.72(3)	86.06(10)	89.9(1)	90.24(13)
S1-Ni-N2	173.14(7)	102.5(3)	174.90(3)	177.61(10)	170.9(1)	163.74(11)
S2-Ni-N1	172.28(9)	174.3(3)	175.00(3)	174.96(10)	170.3(1)	163.74(11)
S2-Ni-N2	88.26(8)	86.7(3)	88.57(3)	86.30(10)	89.1(1)	90.24(13)
N1-Ni-N2	97.3(1)	97.0(4)	95.77(4)	96.32(14)	88.3(2)	87.6(2)
O1-Ni-S1	80.3(3)		89.69(10)			
O1-Ni-S2	83.8(2)		83.83(9)			
O2-Ni-S1	166.1(3)		82.06(9)			
O2-Ni-S2	83.6(2)		89.78(9)			
O2-Ni-N1	91.9(4)		94.12(13)			
O2-Ni-N2	91.4(4)		97.78(13)			
O2-Ni-O1	85.8(3)		169.46(12)			
N1-Ni-O1	92.4(4)		91.84(12)			
N2-Ni-O1	170.3(4)		90.19(13)			

Equivalent atoms generated by symmetry transformations.

Complex **1**[97] and **9**[98] have been previously studied by X-ray crystallography. Complex **2** (**Figure 2**) and **10** (**Figure 3**) are novel. A comparison of the crystal structures of **1** and **2**, and that of **9** and **10** show that there is very little difference in bond lengths and angles when a methyl group is placed on the carbon *alpha* to the thiolates. A slight opening of the S1-Ni-S1 angle and a slight closing of the N1-Ni-N2 angle is observed. The most striking difference between complexes **1** and **9** is in the N-methyl groups: In **1** they are *cis* in configuration, (axial to the N1, N2, C3, C5 plane) whereas in **9** they are *trans* (to the N1, N2, C4, C5 plane), a result of the steric requirements of a five-membered ring, and the tetrahedral requirement of the nitrogen atoms. The S-Ni-S bond angles in complex **1** and **2** are more acute (by about 9°) compared to the corresponding angles in complex **9** and **10**. Conversely the N-Ni-N angle in complex **1** and **2** are more obtuse (by about 9°) compared to the corresponding angles in **9** and **10**. These angular differences would be expected given the smaller chelate bite angle of the 'ethyl strap' in complex **9**.

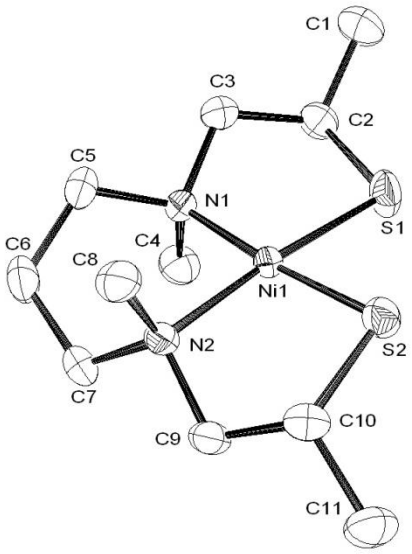

Figure 2: ORTEP plot of complex **2**, ellipsoids at 50% probability. The H atoms have been excluded for clarity. Full structural details are given in **SI (#2)**.

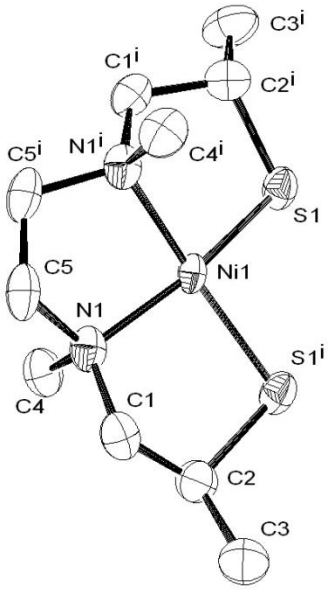

Figure 3: ORTEP plot of complex **10**, ellipsoids at 50% probability. The H atoms have been excluded for clarity. Full structural details are given in **SI (#6)**.

Complexes 3 and **6:** The alkylation of complex **1** or **2** with two equivalents of iodoacetamide gives complex **6** or **3**, respectively (see **SI #1**). These alkylated complexes are high spin (S = 1) dications, blue to purple in color, with pseudo octahedral Ni(II) centers, each with a $N_2S_2O_2$ donor ligand set, and iodide counterions. The iodoacetamide derivatives were readily crystallized (as beautiful gems) from MeOH/MeCN solutions and are very stable in the solid state. ORTEP plots of the crystal structures are shown in **Figures 4** and **5**.

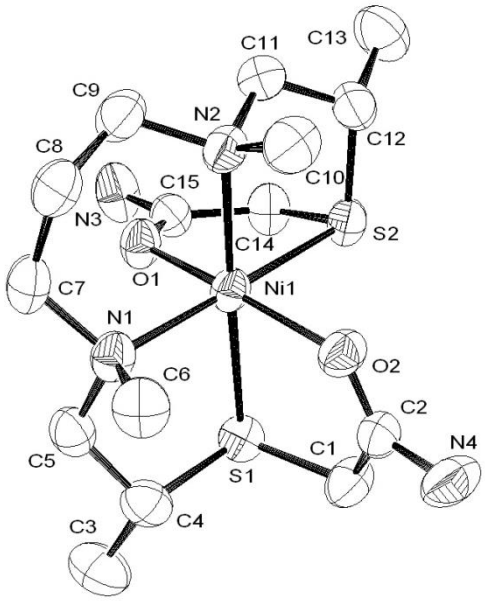

Figure 4: ORTEP plot of complex **3**, ellipsoids at 50% probability. The H atoms and the two iodide counterions have been excluded for clarity. Full structural details are given in **SI (#3)**.

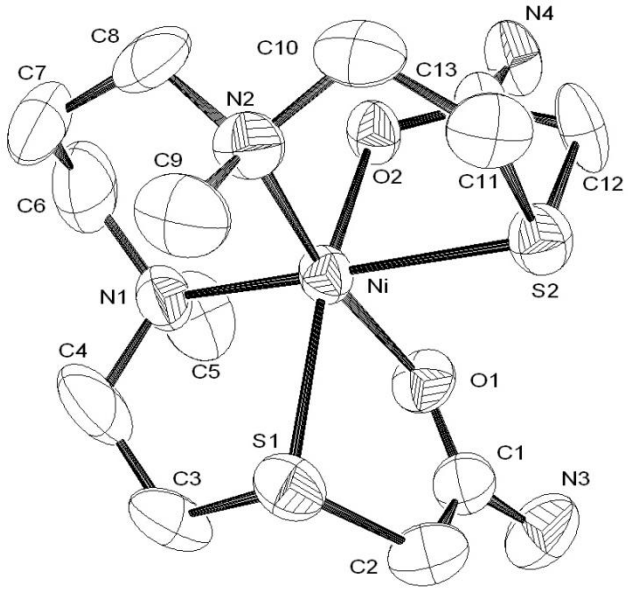

Figure 5: ORTEP plot of complex **6**, ellipsoids at 50% probability. The H atoms and the two iodide counterions, have been excluded for clarity. Full structural details are given in **SI (#4)**.

The most notable structural difference between the iodoacetamide derivatives is that complex **6** contains Ni(II) with a *cis*-*cis*-*cis* geometrical $N_2S_2O_2$ donor ligands, whereas complex **3** contains *cis*-*cis*-*trans* geometry with the O's being *trans*: These large atomic rearrangements, in going from 4 to 6 coordinate avoids *cis* configuration of the N-methyl groups. The expansion of the coordination sphere also leads to expansion of all Ni-N and Ni-S bond lengths. The most pronounced is that for

the Ni-S bonds, which (on average) goes from 2.17 Å to 2.43 Å, this is similar to that observed by others in the literature for a similar Ni(II) environment.[99]

Complexes 4 and **7:** Both of these neutral high spin complexes were synthesized according to published procedures.[100,101] These Schiff base complexes are hydrolytically stable over a wide pH range, due in part to the 5-6-5 membered chelate rings.[100,102,103] The only significant difference between complexes **4** and **7** is the presence of a hydroxyl group on the second carbon of the NN' propyl strap, it is expected that the additional feature will enhance the polar solubility of complex **7**.

Complexes 5, **11**, and **12:** The synthesis of each of these high spin Ni(II) amine/ammine complexes is well documented. Each of the complexes is very soluble in polar solvents, intensely colored, and make for an interesting comparison with the other complexes in this series. Complex **5** is neutral, and complexes **11** and **12** are dications in solution.

Complex 8: The key role of the Ni(II) complex of EDTA in our studies is that it is anionic. The complex is stable and X-ray diffraction studies suggest that the complex in the solid state is a quinquedantate octahedral complex, with one non-complexed protonated acetate, and a water molecule bonded to the Ni. The structure, as shown in **Figure 6**, is similar to that reported in early literature,[104] however some differences are noticeable [*as would be expected 52 years later*], and for that reason an updated crystal structure is presented here. A careful study of the packing relations between molecules strongly indicates that hydrogen bonding contributes significantly to the stability of the crystal.

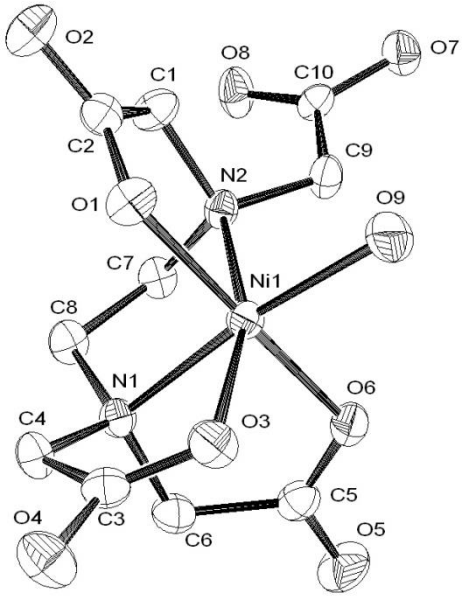

Figure 6: ORTEP plot of complex **8** monoanion, ellipsoids at 50% probability. The H atoms and the Na^+ counterion, have been excluded for clarity. The ligand labeled O9 is water. Full structural details are given in **SI (#4)**.

B. Fluorescence Quenching by Nickel complexes

The fluorescence quenching observed in our studies is a result of the interaction between the ligand that is bound to the Ni complex, the Trp residue and its immediate vicinity in the protein. **Table 2** lists the Trp environment in the proteins studied. The extent of quenching observed varied with protein and with complex, and can be narrowed to some key factors: (i) the hydrophobicity of the ligand, (ii) presence or absence of complex charge, and (iii) the nature of the amino acids surrounding the Trp. While it has been reported in the literature that Ni ions can bind to BSA and form either square planar or octahedral complexes,[28] the quenching observed is dependent on the nature of the ligand.

Table 2: Trp environments in BSA, HSA and Lysozyme.[105] Tyr residues are partially hydrophobic.

		Surrounding Amino Acid Residue(s)			
Protein	**Trp Residue(s)**	**Positively Charged & amphipathic**	**Negatively Charged**	**Polar-Uncharged**	**Hydrophobic**
BSA	Trp-134	-	Glu	Ser	Tyr, Val
	Trp-212	-	-	-	Tyr, Leu, Phe
HSA	Trp-214	-	-	-	Tyr, Val
Lyso	Trp-28	Lys	-	Asn, Thr	Val
	Trp-62,63	Arg	-	Ser	
	Trp-108	-	-	Asn, Gln, Thr	Val
	Trp-111	Arg	Glu	Asn	
	Trp-123	-	-	-	Ile

A typical plot of Trp fluorescence quenching with increasing complex concentration is shown in **Figure 7**. In this case (BSA with complex **2**), the fluorescence decreases by approximately 26% at the highest complex concentration used. The fluorescence quenching ranged from 0-56% in this study (**Table 3**), with the upper limit being slightly lower than the 60% quenching observed in our recently reported study with a Cr(III) complex.[76]

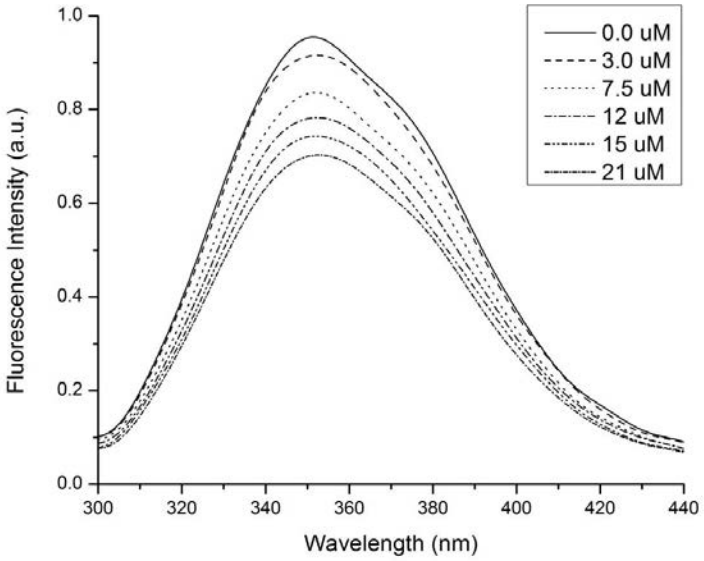

Figure 7: Fluorescence spectra of BSA (1.0×10^{-5} M) in the presence of different concentrations of complex **2**.

Two common mechanisms for fluorescence quenching are dynamic quenching and static quenching. In order to determine the type of quenching taking place, two approaches are available and commonly used: The first involves a temperature-dependent study, as diffusion increases at higher temperatures, collisional quenching and subsequent dissociation of weakly bound complexes leads to a decrease in static quenching. In the second approach, *as used in this work*, the linearity of the Stern-Volmer plot is interpreted. The Stern-Volmer plot of F_0/F against [Q] should be linear (**equation 1**), and this is usually the case for gas-phase and liquid-phase systems where either k_q or τ_0 is large. In the case of the proteins and free Trp, τ_0 is small (10^{-8} to 10^{-9} s), which leads to Stern-Volmer plots that curve upwards.[67,76] Sample plots for BSA quenching by complex **4** are given in **Figure 8**. The dynamic quenching plot (**Figure 8B**) is curving slightly upward even at low complex concentrations. The deviation from linearity is more prominent at higher complex concentrations as illustrated in the case of lysozyme and complex **4** (**Figure 9**). For static quenching, the binding constant (K_a) for the formation of an adduct between the Ni(II) complexes and BSA was determined using a double logarithmic plot (**Figure 8A**). The binding site values (n) were also determined from the slope using **equation 3**.

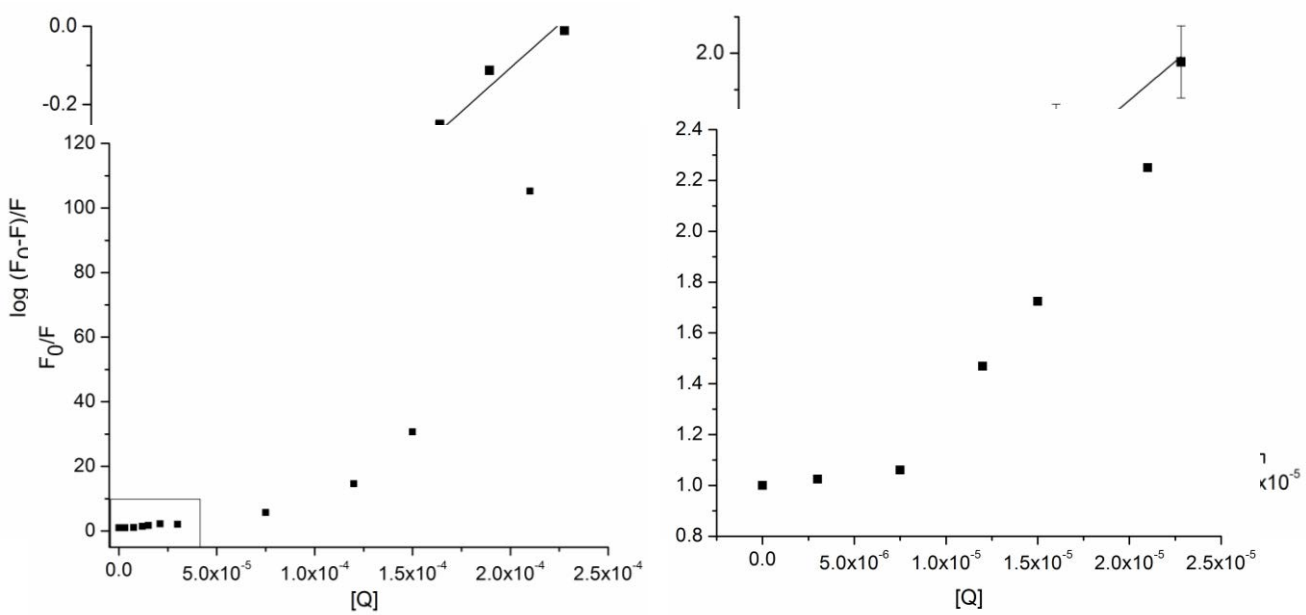

Figure 8: Stern-Volmer plots for (**A**) static quenching ($R^2 = 0.993$) and (**B**) dynamic quenching of BSA by complex **4** ($R^2 = 0.9884$).

Figure 9: Dynamic quenching plot for lysozyme (1.0×10^{-5} M) quenching by complex **4**. (**A**) The fluorescence of the protein is fully quenched when [**4**] approaches 120 μM. (**B**) Expansion of the enclosed area in **A**. Deviation from linearity is evident at complex concentration less than 21 μM.

Another important consideration is that for dynamic quenching, the maximum value of k_q is normally in the range of 2.0×10^{10} $M^{-1}s^{-1}$. [28,73,105] However, in this study, we found values of k_q that are in the order of 10^{12} to 10^{13} $M^{-1}s^{-1}$, which are surprisingly consistent with our recent study involving a Cr(III) complex where a value of 1.8×10^{13} $M^{-1}s^{-1}$ was determined.[76] These large Stern-Volmer constants strongly suggest that static quenching is predominant in these systems. Even though the evidence points towards static quenching, the K_{SV} and k_q values merit some discussion: The k_q values provide a sensitive measure of the exposure of Trp residues in proteins. A low k_q value indicates that the protein is sterically shielding the Trp from the solvent.[13,67,74] In the systems we have studied, that clearly isn't the case as the k_q values are much greater. The k_q values reported in this work are in good agreement with values reported in the literature for BSA-baicalin (~1.7×10^{13} $M^{-1}s^{-1}$), BSA-kaempferol (~8.5×10^{12} $M^{-1}s^{-1}$) and BSA-$[Cr(salprn)(H_2O)_2]^+$ (~1.9×10^{12} $M^{-1}s^{-1}$).[13,74,106] Fluorescence quenching is often a result of energy transfer from a donor (Trp) to an acceptor (metal complex).[74] However, in all the systems and combinations studied, the quenching of Trp fluorescence is static and Forster's long-range energy transfer is not taking place. Also, the spectral overlap between Trp emission and complex absorption is negligible (**Figure 10**) compared to other systems.[45,72,73,76,106] The presence of an overlap between the emission band of the donor and the absorption band of the acceptor is a requirement for FRET. Therefore, the Ni(II) complexes are quenching the fluorescence *via* a thermodynamically favorable ($\Delta G < 0$) interaction with a high binding constant.

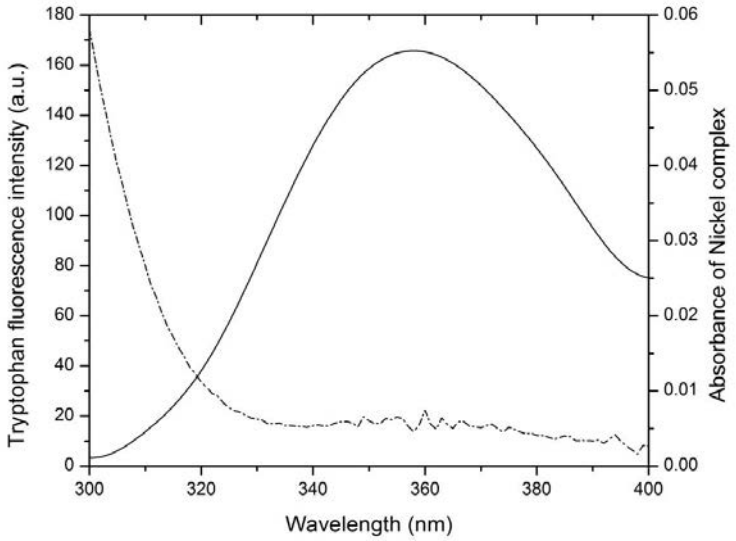

Figure 10: Overlap of Trp emission of 1.0 x 10^{-5} M Trp (solid line) with the absorption of 1.0 x 10^{-5} M complex **1,** showing negligible absorbance of the complex in the region of Trp fluorescence emission.

C. Nature of the Interaction between the proteins and nickel complexes

The proteins used in this study have complex structures and therefore many types of interactions are possible between the protein and a small complex or molecule. Van der Waals, electrostatic, hydrophobic and hydrogen bonding interactions are all possible.[106] The resulting fluorescence quenching of Trp occurs only when there is interaction with the hydrophobic ligands, and the interaction is either promoted or stabilized by the surrounding amino acid residues (**Table 2**).

The most noticeable correlation from data in **Table 3** is that small neutral alkyl Ni(II) complexes (**1**, **2**, **9** and **10**) quench fluorescence better than the bulky charged complexes, such as **3**, **6**, and **8**. The spin state (high spin for the hexacoordinate, and low spin for the tetracoordinate complexes) appears to play little part in the interaction. The hexacoordinate complexes studied are for the most part charged, and only complexes **4**, **5** and **7** are neutral. Of these three neutral complexes, **4** and **7** possess hydrophobic aromatic ligands and are amongst the strongest fluorescence quenchers. The significant decrease in quenching observed between BSA and lysozyme with complex **7** is due to hydrogen-binding interactions resulting from the presence of an OH group in **7**. The high binding constants (K_a) correlate with the negative values obtained for ΔG, confirming that binding is spontaneous. Similar values have been observed in other studies involving BSA, HSA and lysozyme.[45,46,72,73,76,106-108] The ΔH value is zero for hydrophobic interactions, and so ΔS is positive. ΔG values range from -5 to -40 kJ mol^{-1} when one binding site is involved (n = 1), and previous studies[76] have yielded values in the 15 to 35 kJ mol^{-1} range. When more than one binding site is involved, the association is even more thermodynamically favorable, with ΔG from -40 to -60 kJ mol^{-1}.

Table 3: Percent decrease in fluorescence intensity of fluorophore (1.0 x 10^{-5} M) after addition of highest amount of quencher (21 μM).

Protein	Nickel Complexes											
	1	**2**	**3**	**4**	**5**	**6**	**7**	**8**	**9**	**10**	**11**	**12**
BSA	17.2	26.3	No	49.4	No	No	No	No	43.4	31.3	No	No
HSA	20.3	23.7	13.0	54.5	No	No	40.6	No	48.3	28.4	No	No
Lyso	17.2	21.1	No	55.6	No	No	19.3	No	43.3	41.3	No	No
Trp	22.1	No	No	55.9	No	No	36.5	No	48.0	42.0	No	No
Charge on Complex	0	0	+2	0	0	+2	0	-1	0	0	+2	+2

i. BSA and HSA: Both serum albumin proteins were quenched by complexes **1**, **2**, **9** and **10**. These complexes are similar in structure, with what appear to be subtle differences. The binding constants, K_a, for these four complexes were on the order of 10^3 and higher. The fluorescence quenching by complex **9** was the greatest in this group (**Table 3**, 43% for BSA and 48% for HSA) and the K_a values were as high as 10^7, indicating strong binding by this particular complex to the Trp region of the proteins (**Table 4**). Complex **9**, with its 5-5-5 membered chelate rings, is slightly smaller than complexes **1**, **2** and **10** thereby lending itself to a slightly stronger interaction with the protein. The quenching by the slightly larger complex **10** was significantly lower at 30%, with K_a values on the order of 10^4-10^5. For complex **2**, the quenching was about 25% in both cases, and the K_a values were on the order of 10^4 to 10^5. A correlation between complex size and the ability to quench and bind strongly is evident.

Table 4: Summary of binding constant, K_a, binding site number, n, and ΔG for BSA and HSA.

Complex	BSA			HSA		
	K_a, M^{-1}	n	ΔG, kJ mol^{-1}	K_a, M^{-1}	n	ΔG, kJ mol^{-1}
1	3.2×10^4	1	-26	5.7×10^9	2	-56
2	2.7×10^5	1	-31	1.4×10^4	1	-24
3	-	-	-	9.1×10^4	1	-28
4	3.2×10^5	1	-31	2.2×10^5	1	-30

5	-	-	-	-	-	-
7	-	-	-	1.8×10^5	1	-30
9	3.8×10^7	1.5	-43	1.3×10^7	1.5	-41
10	5.8×10^5	1	-33	2.4×10^4	1	-25

A close examination of the immediate environment of each Trp (**Table 2**) indicates that there is at least one hydrophobic or partially hydrophobic or amphiphilic amino acid in the immediate vicinity. In both BSA and HSA, the partially hydrophobic Tyr is buried in the hydrophobic core. Hydrophobic amino acids such as Leu and Val are capable of recognizing and binding hydrophobic ligands. The Tyr residue is also capable of interacting with ligands *via* stacking interactions, which appears to be the nature of the interaction with the pyridinium rings in complexes **4** and **7**. In the case of complex **4**, the fluorescence quenching is the greatest (> 49 %) and the binding constants are on the order of 10^5. Interestingly, HSA showed a strong association with complex **7** ($K_a \sim 10^5$) but BSA did not. The ligand in complex **7** differs from complex **4** in only one regard, it contains an OH group. Trp-134 in BSA has a polar amino acid (Ser) in its vicinity and so it is possible that H-bonding interaction occurs between this residue and complex **7**, in addition to the H-bonding involving Trp. The H-bonding interaction is stronger than any stacking interaction that would be expected between Tyr (or Trp) and the pyridinium group(s) in the complex. The H-bonding between the OH group in the complex and the Ser (and/or Trp) residue is also stronger than hydrophobic interactions promoted by the Leu and Val residues that are in the vicinity of Trp-134. This rationale explains the absence of fluorescence quenching and absence of binding of complex **7** to BSA. On the other hand, HSA does not have a polar amino acid near its Trp-214 so the hydrophobic interactions predominate, leading to fluorescence quenching.

HSA weakly interacts with the neutral complexes **1** and **2** (about 20% quenching), very weakly with the cationic complex **3** (13% quenching), and not at all with complex **6**. These weak or non-existent interactions with **3** and **6** are most likely due to the presence of NH_2 groups in the respective ligands, the interaction with Trp-214, and the influence of the nearby tyrosine residues in HSA. Once again, H-bonding is possible between the NH_2 groups and the amino acids. No interaction was detected for **3** and **6** with BSA due to the presence of more hydrophobic groups, and of course the lower hydrophobicity of the ligands in these complexes.

No fluorescence quenching was observed for any proteins with complexes **11** and **12**. The ligands on complexes **11** and **12** are strongly hydrophilic, and therefore not exhibiting the type of interaction that would lead to quenching of protein fluorescence. In general, interaction between complexes and proteins occurred only with complexes containing hydrophobic ligands. This observation underscores the nature of the Trp residue, and the importance of the immediate vicinity being occupied by one or more hydrophobic residues, or at least partially hydrophobic amino acid residues.

ii. Lysozyme: Lysozyme fluorescence was quenched by complexes **1**, **2**, **4**, **7**, **9** and **10**. These are all neutral complexes, with hydrophobic ligands. Significant quenching was observed with complex **4**. Given that lysozyme has six Trp residues, a variety of interactions are possible between the protein and the Ni(II) complexes. Trp-28, Trp-62, Trp-63 and Trp-111 are close to amphiphilic amino acids like Lys and Arg, while Trp-108 and Trp-123 are close to hydrophobic Val and Ile, respectively. The hydrophobic interactions are the most important. In terms of binding constants, the interaction between lysozyme and complex **4** was exceptionally strong while the interaction with **7** was the weakest (**Table 5**). The ligand in complex **7** differs from **4** in only one regard in that it contains an OH group, which leads to a disruption in binding and quenching. There was no change in fluorescence intensity when 3.0 μM of complex **4** was added but further addition of the complex resulted in significant static quenching over the 3.0 to 21 μM range (**Figure 9**). The high fluorescence quenching resulted in a higher than average binding constant (~10^{10}) and a binding site number of 2.

Table 5: Summary of binding constant, K_a, binding site number, n, and ΔG for lysozyme and free Trp.

Complex	**Lysozyme**			**Free Trp**		
	K_a, M^{-1}	n	ΔG, kJ mol^{-1}	K_a, M^{-1}	n	ΔG, kJ mol^{-1}
1	6.7 x 10^7	2	-45	1.4 x 10^3	1	-18
2	5.1 x 10^7	2	-44	-	-	-
4	1.6 x 10^{10}	2	-58	2.0 x 10^5	1	-30
7	-	-	-	4.6 x 10^2	1	-15
9	5.4 x 10^6	1.5	-38	9.8 x 10^4	1	-28
10	2.8 x 10^5	1	-31	2.4 x 10^5	1	-31

iii. Free tryptophan: Free Trp showed very similar behavior towards the Ni(II) complexes as the three proteins. The interaction was strongest with neutral complexes **1**, **4**, **7**, **9** and **10** (**Table 5**). The absence of quenching with complex **2** is anomalous, and could be attributed to the steric effects resulting from the slightly larger size of the ligand when compared to the alkyl ligands in complexes **1**, **9** and **10**. The interaction with **7** is significantly weaker due to the presence of the OH group on the ligand in the complex. This observation opens up the possibility of non-hydrophobic interactions taking precedence over hydrophobic interactions between the Trp and the pyridinium groups in the complex. This is similar to what was observed with BSA where there was no interaction with **7**, but a strong interaction with **4**.

Our data suggests that in most of the systems studied, one binding site is present in each, the exceptions include all the interactions with lysozyme (except with complex **10**), HSA with complex **1** (n = 2), HSA with complex **9** (n = 1.5), and BSA with complex **9** (n = 1.5). A binding site number of 1 is typical when static quenching of proteins occurs as a result of hydrophobic interactions with

transition metal complexes and other molecules. The presence of two binding sites in lysozyme is not unusual as there are six Trp residues in the protein, and complex **4** can associate with the different Trp residues *via* stacking interactions through the pyridinium groups. The small size of complexes **1**, **2** and **9** is also an important factor, allowing for these complexes to squeeze in to additional bindings sites. Complex **9** is the smallest of these complexes, and is found to be binding more strongly to both BSA and HSA compared to any of the other complexes, therefore a higher binding site number is not unexpected. BSA has two and HSA has only one Trp residue, and so the presence of two binding sites in HSA raises the possibility that multiple small quencher molecules may be involved since they would have easy access to the Trp residue *via* hydrophobic interactions.

Quantum chemical computational studies using *ab initio* methods (Gaussian09) are currently underway to determine the energetic contribution of the interactions between the Trp residues and the surrounding amino acids in HSA, BSA, and lysozyme, with these Ni(II) complexes.

CONCLUSIONS

We have synthesized and fully characterized a series of Ni(II) complexes. Fluorescence quenching studies with albumins and lysozyme proteins clearly suggests that the Ni(II) complexes featuring hydrophobic ligands exhibit strong and favorable interactions. These interactions takes place between the hydrophobic pocket of the protein and the ligand. The poorest interactions are with charged bulky Ni(II) complexes. Static quenching was found to be the predominant form of quenching taking place in these systems, and generates high binding constants. The small neutral square planar Ni(II) complexes (**1**, **2**, **9** and **10**) and the neutral aromatic complexes (**4** and **7**) are currently being studied as possible DNA intercalators and quadruplex DNA promoters.

ACKNOWLEDGEMENTS

We are grateful to Dr. Carl Carrano and Mr. J. Hoffman at San Diego State University, Dr. H. Yennawar at Penn State University, and Dr. A. Chandrasekaran at UMass-Amherst for help with the single crystal crystallographic studies. We thank Susquehanna University and Penn State Harrisburg for financial support for this project.

REFERENCES

1. H. J. Bohm, *Protein-ligand Interactions: From Molecular Recognition to Drug Design.* Wiley VCH, Weinheim, 2003.
2. H.-J. Schneider, *Ang Chem Int Ed*, 2009, **48**, 3924-3977.
3. H. Vorum, K. Fisker and B. Honore, *J Pept Res*, 1997, **49**, 347-354.

4. G. Zolese, G. Falcioni, E. Bertoli, R. Galeazzi, M. Wozniak, Z. Wypych, E. Gratton and A. Ambrosini, *Proteins*, 2000, **40**, 39-48.
5. J. P. Laussac and B. Sarkar, *Biochemistry*, 1984, **23**, 2832-2838.
6. W. Bal, J. Christodoulou, P. J. Sadler and A. Tucker, *J Inorg Biochem*, 1998, **70**, 33-39.
7. A. Sulkowska, B. Bojko, J. Równicka, D. Pentak and W. Sulkowski, *J Mol Struct*, 2003, **651-653**, 237-243.
8. Y. Li, W. He, J. Liu, F. Sheng, Z. Hu and X. Chen, *Biochim Biophys Acta*, 2005, **1722**, 15-21.
9. Y. Q. Wang, H. M. Zhang, G. C. Zhang, W. H. Tao, Z. H. Fei and Z. T. Liu, *J Pharm Biomed Anal*, 2007, **43**, 1869-1875.
10. P. Gosling, *Care Critical*, 1995, **11**, 57-61.
11. T. Peters, Jr., *Adv Protein Chem*, 1985, **37**, 161-245.
12. T. Peters, *All about Albumin: Biochemistry ,Genetics and Medical Applications.* , Academic Press, San Diego, 1995.
13. J. Tian, J. Liu, X. Tian, Z. Hu and X. Chen, *Journal of Molecular Structure*, 2004, **691**, 197-202.
14. T. Peters, *The albumin molecule: Its structure and chemical properties, in All About Albumin. Biochemistry, Genetics And Medical Applications.* , Academic Press, San Diego, 1996.
15. X. M. He and D. C. Carter, *Nature*, 1992, **358**, 209-215.
16. D. C. Carter and X. M. He, *Science*, 1990, **249**, 302-303.
17. D. C. Carter, X. M. He, S. H. Munson, P. D. Twigg, K. M. Gernert, M. B. Broom and T. Y. Miller, *Science*, 1989, **244**, 1195-1198.
18. K. Kim and W. Kauzmann, *J Phys Chem*, 1980, **84**, 163-165.
19. H. C. Tai, Thesis, University of Saskatchewan, Saskatoon, Canada, 2004.
20. D. C. Carter, B. Chang, J. X. Ho, K. Keeling and Z. Krishnasami, *Eur J Biochem*, 1994, **226**, 1049-1052.
21. Carter, D. C.; and Ho, J. X., *Adv. Protein Chem.* 1994, **45**, 153.
22. Curry, S.; Brick, P.; and Frank, N. P., *Biochim Biophys Acta.* 1999, **1441**, 13125.
23. Petitpas, I.; Grune, T.; Battacharya, A. A.; and Curry, S., *J. Mol. Biol.* 2001;314:955.
24. Grelamo, E. L.; Silva, C. H. T. P.; Imasato, H.; and Tabak, M., *Biochim Biophys Acta.* 2002, **1594**, 84.
25. V. Lhiaubet-Vallet, Z. Sarabia, F. Bosca and M. A. Miranda, *J Am Chem Soc*, 2004, **126**, 9538-9539.
26. M. C. Jimenez, M. A. Miranda and I. Vaya, *J Am Chem Soc*, 2005, **127**, 10134-10135.
27. J. Koch-Weser and E. M. Sellers, *New Eng J Med*, 1976, **294**, 526-531.
28. S. H. Laurie and D. E. Pratt, *J Inorg Biochem*, 1986, **28**, 431-439.
29. E. Nieboer, R. T. Tom and W. E. Sanford, *Metal ions in biological systems: Nickel and its role in biology.*, Dekker, NY, 1988.
30. J. D. Glennon and B. Sarkar, *Biochem J*, 1982, **203**, 15-23.
31. W. M. Callan and F. W. Sunderman, Jr., *Res Commun Chem Pathol Pharmacol*, 1973, **5**, 459-472.
32. R. W. Hay, M. M. Hassan and C. You-Quan, *J Inorg Biochem*, 1993, **52**, 17-25.
33. E. L. Giroux and R. I. Henkin, *Biochim Biophys Acta*, 1972, **273**, 64-72.
34. E. Ohyoshi, Y. Hamada, K. Nakata and S. Kohata, *J Inorg Biochem*, 1999, **75**, 213-218.
35. E. Giroux and J. Schoun, *J Inorg Biochem*, 1981, **14**, 359-362.
36. W. Goumakos, J. P. Laussac and B. Sarkar, *Biochem Cell Biol*, 1991, **69**, 809-820.
37 J. C. Vidal, G. Cepria and J. R. Castillo, *Anal Chim Acta*, 1992, **259**, 129-138.
38. J. Masuoka, J. Hegenauer, B. R. Van Dyke and P. Saltman, *J Biol Chem*, 1993, **268**, 21533-21537.
39. J. Masuoka and P. Saltman, *J Biol Chem*, 1994, **269**, 25557-25561.
40. P. J. Sadler and J. H. Viles, *Inorg Chem*, 1996, **35**, 4490-4496.
41. Y. Zhang and D. E. Wilcox, *J Biol Inorg Chem*, 2002, **7**, 327-337.
42. Z. Yongqia, H. Xuying, D. Chao, L. Hong, W. Sheyi and S. Panwen, *Biophys Chem*, 1992, **42**, 201-211.
43. H. Liang, J. Huang, C. Q. Tu, M. Zhang, Y. Q. Zhou and P. W. Shen, *J Inorg Biochem*, 2001, **85**, 167-171.
44. E. G. Ferrer, A. Bosch, O. Yantorno and E. J. Baran, *Bioorg Med Chem*, 2008, **16**, 3878-3886.

45. Q. Wei, D. Wu, B. Du, Y. Li and C. Duan, *Spectrochim Acta A Mol Biomol Spectrosc*, 2006, **63**, 532-535.
46. Y. Zhang, Z. Qi, D. Zheng, C. Li and Y. Liu, *Biol Trace Elem Res*, 2009, **130**, 172-184.
47. C. Harford and B. Sarkar, *Acc Chem Res*, 1997, **30**, 123-130.
48. J. Christodoulou, P. J. Sadler and A. Tucker, *Eur J Biochem*, 1994, **225**, 363-368.
49. B. P. Espósito and R. Najjar, *Coord Chem Rev*, 2002, **232**, 137-149.
50. L. Trynda-Lemiesz, H. Kozlowski and B. K. Keppler, *J Inorg Biochem*, 1999, **77**, 141-146.
51. N. E. Dixon, T. C. Gazzola, R. L. Blakeley and B. Zermer, *J Am Chem Soc*, 1975, **97**, 4131-4133.
52. S. Nomoto, M. D. McNeely and F. W. Sunderman, Jr., *Biochemistry*, 1971, **10**, 1647-1651.
53. E. Denkhaus and K. Salnikow, *Crit Rev Oncol Hematol*, 2002, **42**, 35-56.
54. G. M. Gadd, *FEMS Microbiol Lett*, 1992, **79**, 197-203.
55. S. Zhicheng, Y. Zhiming, A. Lata and H. Yuhua, *Br J Ind Med*, 1986, **43**, 642-643.
56. J. P. Thyssen, A. Linneberg, T. Menne and J. D. Johansen, *Contact Dermatitis*, 2007, **57**, 287-299.
57. B. Roediger and W. Weninger, *Immunol Cell Biol*, **89**, 1-2.
58. M. Schmidt, B. Raghavan, V. Muller, T. Vogl, G. Fejer, S. Tchaptchet, S. Keck, C. Kalis, P. J. Nielsen, C. Galanos, J. Roth, A. Skerra, S. F. Martin, M. A. Freudenberg and M. Goebeler, *Nat Immunol*, **11**, 814-819.
59. H. J. Thierse, C. Moulon, Y. Allespach, B. Zimmermann, A. Doetze, S. Kuppig, D. Wild, F. Herberg and H. U. Weltzien, *J Immunol*, 2004, **172**, 1926-1934.
60. M. Miyazawa, Y. Ito, Y. Yoshida, H. Sakaguchi and H. Suzuki, *Toxicol In Vitro*, 2007, **21**, 428-437.
61. F. Boisleve, S. Kerdine-Romer and M. Pallardy, *Toxicology*, 2005, **206**, 233-244.
62. T. Rustemeyer, I. vanHoogstraten, B. M. von Blomberg and S. R., *Textbook of Contact Dermatitis*, Springer, Berlin, 2001.
63. J. J. Hostynek, F. Dreher, A. Pelosi, A. Anigbogu and H. I. Maibach, *Acta Derm Venereol Suppl, Stockholm*, 2001, 5-10.
64. T. Rabilloud, D. Asselineau and M. Darmon, *Mol Biol Rep*, 1988, **13**, 213-219.
65. Y.-J. Hu, Y. Liu, L.-X. Zhang, R.-M. Zhao and S.-S. Qu, *J Mol Struct*, 2005, **750**, 174-178.
66. J. R. Lakowicz, *Principles of Fluorescence Spectroscopy*, Springer Science, U.S.A., 2004.
67. M. R. Eftink and C. A. Ghiron, *Analytical Biochemistry*, 1981, **114**, 199-227.
68. K. M. Sanchez, D. E. Schlamadinger, J. E. Gable and J. E. Kim, *J Chem Ed*, 2008, **85**, 1253-1256.
69. J. M. Beechem and L. Brand, *Annu Rev Biochem*, 1985, **54**, 43-71.
70. M. R. Eftink and C. A. Ghiron, *Biochemistry*, 1976, **15**, 672-680.
71. M. R. Eftink and C. A. Ghiron, *Anal Biochem*, 1981, **114**, 199-227.
72. D. Wu, B. Du, H. Ma, Q. Wei and G. Xu, *Spec Lett*, 2006, **39**, 399 - 408.
73. D. Wu, Q. Wei, Y. Li, B. Du and G. Xu, *Int J Biol Macromol*, 2005, **37**, 69-72.
74. H. Y. Shrivastava and B. U. Nair, *J Inorg Biochem*, 2004, **98**, 991-994.
75. K. H. Gustavson, *J Am Chem Soc*, 1952, **74**, 4608-4611.
76. H. F. Crouse, E. M. Petrunak, A. M. Donovan, A. C. Merkle, B. L. Swartz and S. Basu, *Spec Lett*, 2011, **44**, 369-374.
77. T. Imoto, L. S. Forster, J. A. Rupley and F. Tanaka, *Proc Natl Acad Sci U S A*, 1972, **69**, 1151-1155.
78. T. Imoto, L. N. Johnson, A. T. C. North, D. C. Phillips and J. A. Rupley, *Lysozyme in Enzymes*, Academic Press, NY, 1972.
79. M. J. Kronman and L. G. Holmes, *Photochem Photobiol*, 1971, **14**, 113-134.
80. M. R. Eftink and C. A. Ghiron, *Proc Natl Acad Sci U S A*, 1975, **72**, 3290-3294.
81. S. S. Lehrer, *Biochemistry*, 1971, **10**, 3254-3263.
82. C. Formoso and L. S. Forster, *J Biol Chem*, 1975, **250**, 3738-3745.
83. M. Eftink, *Biophys J*, 1983, **43**, 323-334.
84. A. J. Gordon and R. A. Ford, *The Chemist's Companion*, J. Wiley and Sons, NY, 1972.
85. J. A. Riddick, W. B. Bunger and T. K. Sakano, *Organic Solvents*, J. Wiley and Sons, NY, 1986.
86. D. H. Grant, *J Chem Ed*, 1995, **72**, 39-40.
87. D. F. Evans, *J. Chem. Soc.*, 1959, 1351.
88. G. Sheldrick, *Acta Cryst Sec A*, 1990, **46**, 467-473.

89. L. Farrugia, *J App Cryst*, 1997, **30**, 565.
90. C. M. Schneck, A. J. Poncheri, J. T. Jennings, D. L. Snyder, J. L. Worlinsky and S. Basu, *Spectrochim Acta A Mol Biomol Spectrosc*, 2010, **75**, 624-628.
91. J. S. Johansson, *J Biol Chem*, 1997, **272**, 17961-17965.
92. R. Swaminathan, G. Krishnamoorthy and N. Periasamy, *Biophys J*, 1994, **67**, 2013-2023.
93. H. M. Rawel, S. K. Frey, K. Meidtner, J. Kroll and F. J. Schweigert, *Mol Nutr Food Res*, 2006, **50**, 705-713.
94. K. D. Karlin and S. J. Lippard, *J Am Chem Soc*, 1976, **98**, 6951-6957.
95. M. A. Turner, W. L. Driessen and J. Reedijk, *Inorg Chem*, 1990, **29**, 3331-3335.
96. H. J. Krueger and R. H. Holm, *Inorg Chem*, 1989, **28**, 1148-1155.
97. G. J. Colpas, M. Kumar, R. O. Day and M. J. Maroney, *Inorg Chem*, 1990, **29**, 4779-4788.
98. Hosler, E. R.; Herbst, R. W.; Maroney, M. J.; and Chohan, B. S., *Dalton Trans.* 11/2011, **DOI: 10.1039/c1dt11032b**.
99. J. J. Smee, D. C. Goodman, J. H. Reibenspies and M. Y. Darensbourg, *Eur J Inorg Chem*, 1999, **1999**, 539-546.
100. T. G. Campbell and F. L. Urbach, *Inorg Chem*, 1973, **12**, 1836-1840.
101. J. L. Corbin, K. F. Miller, N. Pariyadath, S. Wherland, A. E. Bruce and E. I. Stiefel, *Inorg Chim Acta*, 1984, **90**, 41-51.
102. D. C. Weatherburn, E. J. Billo, J. P. Jones and D. W. Margerum, *Inorg Chem*, 1970, **9**, 1557-1559.
103. Y. Nakao, H. Ishibachi and A. Nakahara, *Bull. Chem. Soc. Jap.*, 1970, 43.
104. G. S. Smith and J. L. Hoard, *J Am Chem Soc*, 1959, **81**, 556-561.
105. K. I. Sugae and B. Jirgensons, *J Biochem*, 1964, **56**, 457-464.
106. J. B. Xiao, J. W. Chen, H. Cao, F. L. Ren, Y. Yang, C. S. Chen and M. Xu, *J Photochem Photobiol A: Chemistry*, 2007, **191**, 222-227.
107. H. Wu, S. S. Lian, Y. and Y. Wan, *Anal Sci*, 2007, **23**, 419-422.
108. J. Tian, J. Liu, X. Tian, Z. Hu and X. Chen, *J Mol Struct*, 2004, **691**, 197-202.